(Received 23 November 2024, Accepted 7 January 2025, Scheduled 16 January 2025)

Wideband MIMO Antenna System with High Inter-Elements Isolation for mm-Wave Communications and the Internet of Things (IoT)

Ijaz Ahmad[1, 2, 3, 4], Yuhuai Liu[1, 2, 3, 4, *], Fang Wang[1, 2, 3, 4], Muhammad K. Khan[5], and Mian Muhammad Kamal[6]

[1] *National Center for International Joint Research of Electronic Materials and Systems International Joint-Laboratory of Electronic Materials and Systems of Henan Province School of Electrical and Information Engineering, Zhengzhou University, Zhengzhou, Henan 450001, China*
[2] *International Joint Laboratory for Integrated Circuits Design and Application, Ministry of Education School of Physics, Zhengzhou University, Zhengzhou 450052, China*
[3] *Institute of Intelligence Sensing, Research Institute of Industrial Technology Co. Ltd. Zhengzhou University, Zhengzhou, Henan 450001, China*
[4] *Zhengzhou Way Do Electronics Co. Ltd., Zhengzhou, Henan 450001, China*
[5] *Department of Telecommunication Engineering, University of Engineering and Technology, Mardan 23200, Pakistan*
[6] *School of Electronic Science and Engineering, Southeast University, Nanjing 210018, China*

ABSTRACT: A four-port, extremely wideband MIMO array antenna is designed for 5G applications. A single element antenna composed of a two-ring-shaped patch with a partial ground plane is designed. It is then converted into a 1×2 array, four arrays of such are placed orthogonally to each other in a MIMO system to get good isolation among them. A Roger substrate with permittivity of 2.2, loss tangent of 0.0009, and thickness of 0.254 mm is used. The antenna arrays of the MIMO system operate in the range from 24 GHz to 51 GHz with good isolation of more than 22 dB. The peak gain of the MIMO system is 7.4 dB with a bi-directional radiation pattern and efficiency of more than 96%. Also, the overall size of MIMO antennas is compact, with dimensions $18 \times 18 \times 0.254\,\text{mm}^3$. For further verification, the measurements of the fabricated prototype were carried out as well, and a very reasonable agreement with simulated results was achieved which guaranteed the prototype's strong MIMO performance. The proposed array MIMO system, owing to its various properties, is a potential candidate for mm-wave 5G applications, mm-wave vehicular communication, and the Internet of Things (IoT).

1. INTRODUCTION

An antenna is a vital component in a communication system which enables wireless communication with other devices. The millimeter wave (mm-wave) multiple-input multiple-output (MIMO) antennas have been capable of significantly improving the performance of antennas when being applied to communication systems compared with traditional antennas [1, 2]. Propagation at mm-wave frequencies spectrum is competent in providing more resources to be shared among multiple users. In addition, the limited availability of microwave bandwidth and the extremely busy part of its spectrum also forced a shift towards new spectrum bands that can provide higher data rates [3]. Consequently, 5G wireless communication systems are already being witnessed to use the mm-wave spectrum [1]. Despite that, mm-wave assures huge bandwidth and high data rates with low latency [4], but the role of the antenna's geometrical structure and size cannot be ignored in mm-wave communication systems [5, 6]. Even though microstrip patch antennas are low-profile, compact and easy to fabricate, they are suitable for mm-wave communication systems. However, the major disadvantages of microstrip patch antennas are their limited narrow bandwidth and compromised gain [7]. Many researchers have suggested various antenna designs and approaches to address the issues of insufficient gain and narrow bandwidth in particular. Slots on the patch [8] are introduced to obtain improved bandwidth, reduce the patch size, and enhance efficiency. The bandwidth increases from 1.46 GHz to 2.26 GHz with the establishment of (etching of) two rectangle-shaped slots in the radiating patch of a single-band antenna resonating at 28 GHz [9].

Also, a 28 GHz microstrip patch antenna comprising a U-shaped slot has been suggested in [10]. In [11], the patch antenna resonates at dual frequency bands (28 GHz and 38 GHz) consisting of L-shaped slots around the patch; the L-shaped two opposite slots contribute as a dual-band resonator, widen the bandwidth, and reduce the patch size. The effect of variation of the circular slot incorporated at the center of the patch element has been investigated in [12]. The radius (r) of the inserted circular slot shifts the resonance of the antenna and contributes to obtaining the band of interest, resonating at 28 GHz with a bandwidth of 6 GHz (ranging from 26 GHz to 32 GHz). Furthermore, the geometric shape of the ground plane, such a rectangular, circular, E, H, I, or ring shape is also important

* Corresponding author: Yuhuai Liu (ieyhliu@zzu.edu.cn).

in obtaining the desired resonance [13]. To attain the optimum bandwidth, the ground plane is reduced from full to half ground [14]. Furthermore, the insertion of a slot in the center of the ground plane, along with parametric optimization of the antenna dimensions and the use of a novel technique of augmented ground structure (AGS), transformed the antenna into a dual resonance operation (20.55 GHz–39.75 GHz and 40.32 GHz–50 GHz) wideband antenna [15]. The authors of [16] proposed an antenna design which covers the band 25.1 to 37.5 GHz using a defective ground structure. It is pointed out that the defective ground structure (DGS) method not only increases bandwidth and shifts its resonance frequency for the intended application but also provides simplicity to antenna design [17, 18]. Advancements in technology will require the 5G wireless infrastructure to handle massive data flow due to high-resolution video streaming, internet of things (IoT)-based remote monitoring, virtual reality, real-time-control applications, smart cities, and IoV-based automobiles [19, 20]. These systems require MIMO antennas with a wide bandwidth to enable high data rates. In the MIMO system, the antenna elements are closer to each other. Therefore, mutual coupling among the antenna elements takes place and reduces antenna performance [21]. Multiple decoupling techniques have been adopted to improve MIMO antenna performance, such as DGS achieving high isolation but causing a low front-to-back radiation ratio for big structures [22], electromagnetic band gap (EBG) [23, 24], neutralization line [25, 26], and introducing air gap [27]. However, these techniques are costly and complicated, and the antenna designs get more difficult as antenna size shrinks in the millimeter wave region. Furthermore, in the prior research structures arrangement in MIMO antenna, high isolation between antenna parts might be challenging, making it difficult to provide a wide impedance bandwidth with good port isolation, resulting in decreased system capacity and overall performance [28]. The key considerations for the antenna model encompass compact dimensions, low profile, high isolation, and achieving the maximum available bandwidth. Therefore, the antenna design has to be optimized depending on one's requirements and its usage.

This work presents a single-element structure that supports the wideband. The proposed structure is converted into a linear two-element array to improve the gain. Then, the linear array assembly is transformed into a MIMO configuration, which contributes to enhancing the capacity. The proposed antenna design structure is composed of radiating patches that are orthogonally arranged to reduce the antenna's overall footprint and boost its degree of isolation. Also, the curved shape of the circular patch and circular slots serve to deflect the coupling effect away from the antenna components. This results in reduced coupling between neighboring antenna elements, thereby leading to enhanced isolation between the ports. The approach used to attain the frequency band spectrum specified for 5G millimeter-wave applications is facilitated by optimizing the circular patch and slots size. In order to attain the lower envelope correlation coefficient values, a crucial metric for MIMO antennas, the suggested design as a whole, makes use of the separated partial grounds structure and orthogonal arrangement. The proposed MIMO antenna system exhibits reasonable performances over extremely wide bandwidth, as well as easy expansion to large-scale antenna systems. The proposed antenna design is novel owing to its features of covering very wide bandwidth, simple design, easy fabrication, and cost effectiveness and good achievement of MIMO diversity parameters values. It is well known that IoT will connect various devices in large scale, and to maintain efficient and large-scale communication among devices, wide bandwidth will be the ultimate requirement. The proposed antenna system fulfils this demand. It is a potential candidate for IoT communication.

This work consists of four key stages. The initial step outlines the process of designing the basic single patch element, which is then converted into two two-element array structures and finally to a 4-port MIMO configuration, which operates within a wide millimeter-wave frequency range. The second phase revolves around creating a Multiple-Input Multiple-Output (MIMO) configuration, with a focus on analysing both the simulated and measured S-parameters of the MIMO, along with examining its simulated and measured radiation characteristics, gains, efficiencies, and surface current distributions. Then, moving to the third stage, the diversity performance of the proposed MIMO antenna is presented and explored, including performance indicators such as envelope correlation coefficient (ECC), diversity gain (DG), mean effective gain (MEG), and channel capacity (CCL). In the fourth stage, a comparative study with existing research works is carried out. Finally, the paper is concluded.

2. ANTENNA GEOMETRY

2.1. Single Element Structure

The design of the proposed antenna MIMO arrangement initially starts with the modelling of a single-element patch antenna. The front and back sides of a single element's geometry are depicted in Fig. 1(a).

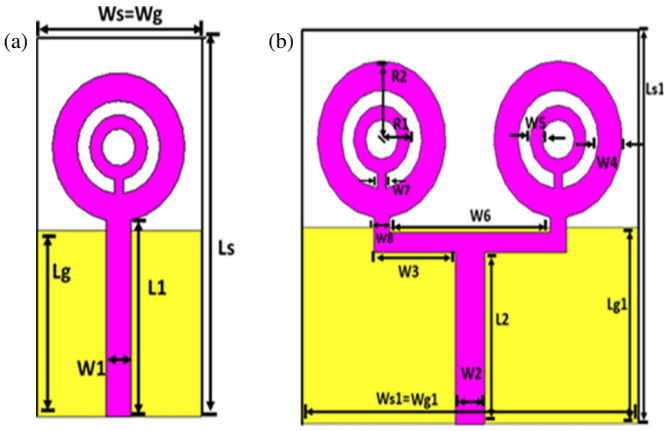

FIGURE 1. Design of (a) single element and (b) 1×2 antenna array.

In order to better understand the proposed design, a simple circular patch element is designed in the first step. The circular patch element is then converted to a ring-shaped structure with an outer radius of 1.6 mm and inner radius of 1 mm in the next step. It is noted that the size of the large circular ring controls the resonance impedance of the proposed structure. As

can be observed from the optimisation illustrated in Fig. 2, for the outer radius equal to 1.8 mm in step 1, the resonance of the radiating patch is at a higher frequency and in step 2 shifted to a comparatively low frequency when the outer radius is selected to be 1.6 mm as shown in Fig. 2.

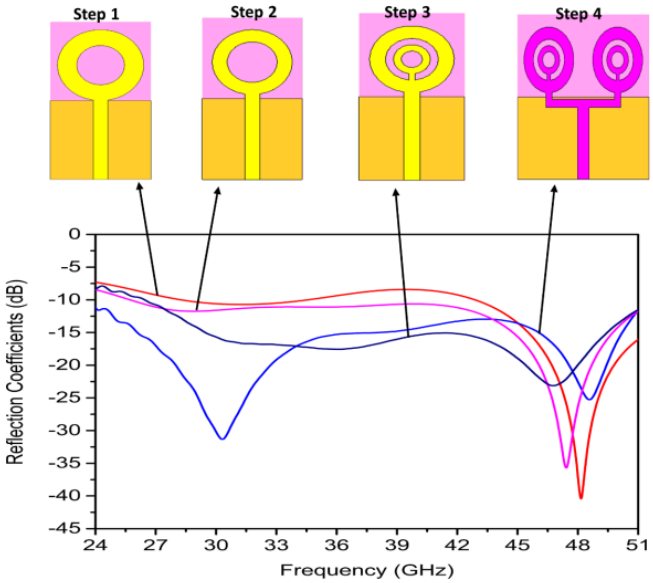

FIGURE 2. Design steps of antenna element.

Finally, another small circular ring-shaped element is placed inside the big ring, and both the rings are connected to the main 50 Ω feed line. The inclusion of a second small circle improves the level of resonating bandwidth, as shown in Fig. 2 by comparing step 3 to step 2 of the design. Also, the second circle increases the effective area of the antenna. In step 4, the single element is converted into a 1 by 2 array, which further improves the impedance matching over the wide band of frequency. The backplane is composed of the partial ground copper plane with a thickness of 0.035 mm, which enhances the performance and helps to achieve wideband radiation patterns within a wide desired frequency range. Besides that, the size of the ground plan is also a key sensitive parameter that influences the input impedance of the monopole antenna. The increase or decrease in length of the partial ground plane significantly affects the bandwidth of the proposed antenna element, as shown in Fig. 3. The proposed geometry is constructed on Rogers RT 5880 substrates with dimensions $8 \times 4 \times 0.254\,\text{mm}^3$, dielectric constant ($\varepsilon_r$) 2.2, and loss tangent 0.0009. The outer radius (R_2) of the circular-shaped patch could be calculated with the help of these parameters by using Equation (1) [29].

$$R_2 = \frac{F}{\sqrt{1 + \frac{2h}{\pi\varepsilon_r F}\left(\ln\left(\frac{\pi F}{2h}\right)\right) + 1.7729}} \tag{1}$$

where

$$F = \frac{8.791 \times 10^9}{f_r\sqrt{\varepsilon_r}}$$

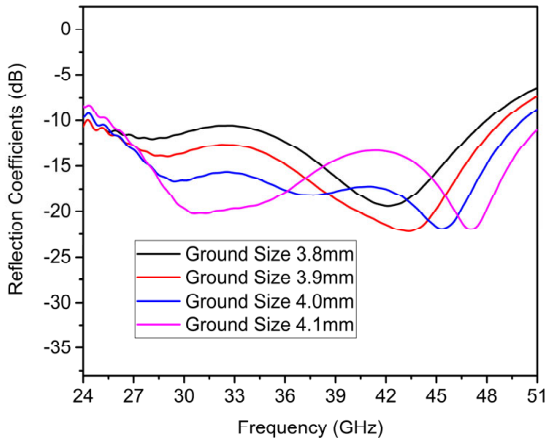

FIGURE 3. Effects of ground plane length on single element structure.

Furthermore, the iteration process is performed by considering different parameters which improved antenna's performance across a wideband frequency range. All simulations are executed using full wave CST software.

2.2. Two Element Antenna Array Structure

In addition, the proposed single patch element antenna is transformed into a two-element array structure given in Fig. 1(b). The array configuration has been adopted to obtain higher gain with a narrow radiation beam pattern. The two-element array significantly increases the gain of a single element antenna. Also, the two-element array structure improved the impedance matching, as compared in Fig. 2.

Corporate feed technique is used, and both the elements of the array are excited by a parallel feed network with a main feed of 50 Ω. The inter-element spacing between the array elements is usually taken to be $\frac{\lambda_0}{2}$ of the wave wavelength of operating frequency. As the proposed design achieves wide bandwidth, the distance between array elements is carefully selected to be 4 mm. The two-element linear array structure, along with its feeding network, is shown in Fig. 1(b). Table 1 provides the design parameter lengths in mm.

TABLE 1. Lengths of the single element and 1×2 array parameters.

Parameter	L_s	W_s	R_1	R_2	W_1	W_2	W_3
Value (mm)	8	4.5	0.7	1.6	0.6	0.7	2
Parameter	W_4	W_5	W_6	W_7	W_8	W_{g1}	L_g
Value (mm)	0.6	0.3	4	0.24	0.4	9	4
Parameter	L_1	L_{g1}	W	L			
Value (mm)	4.2	4	18	18			

2.3. MIMO Antenna System Design

At the end, a 4-port MIMO antenna system is developed to increase the capacity of the antenna array. The MIMO antenna array is small in size with dimensions of $18 \times 18 \times 0.254\,\text{mm}^3$. Each single MIMO element consists of a two-element antenna array. The array elements are placed orthogonal to each other

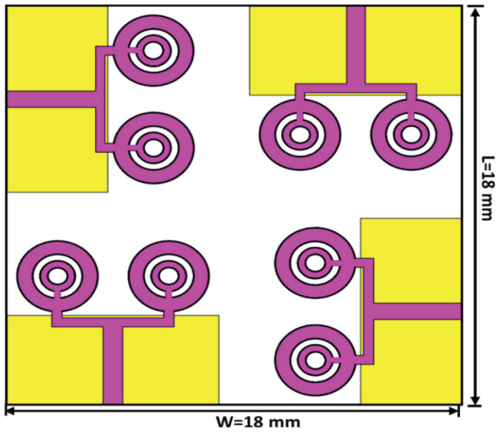

FIGURE 4. Design of four port MIMO antenna array.

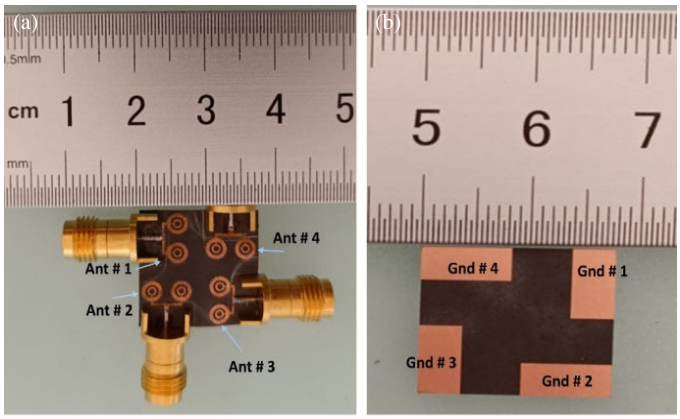

FIGURE 5. Fabricated prototype of the four port MIMO antenna array. (a) Front view. (b) Back view.

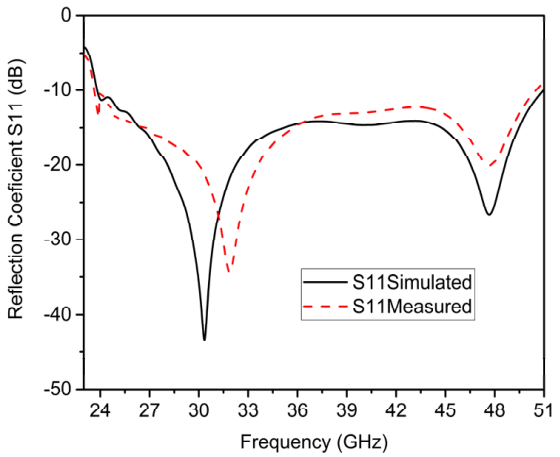

FIGURE 6. Reflection coefficients of arrays in MIMO system.

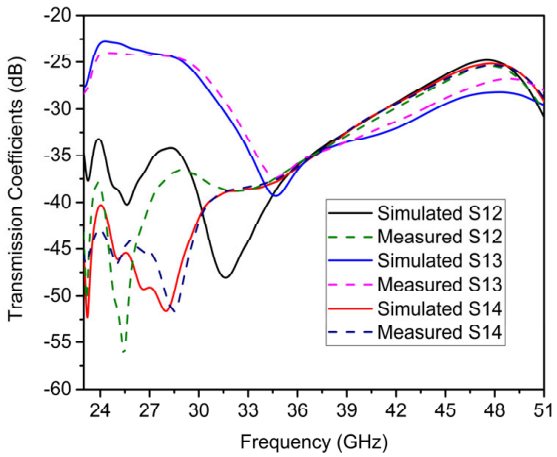

FIGURE 7. Transmission coefficients of arrays in MIMO system.

to attain high isolation. The complete geometry of the proposed mm-wave MIMO antenna array system is shown in Fig. 4 and its prototype in Fig. 5, respectively.

3. RESULTS AND DISCUSSION

3.1. Scattering Parameters

The scattering parameters of a single element, two elements array and 4×4 MIMO antenna system are obtained by simulations in CST software and also measured by using 2.4 mm Female PCB Mount Connector with ZVA 67 Vector Network Analyzer. A good agreement is observed between the simulated and measured results. To obtain extremely wide bandwidth and the reflection coefficient (S_{11}) value less than -10 dB in the entire wide bandwidth, the parametric study is performed, and the optimum parameters of the final single-element antenna are selected. The reflection coefficient (S_{11}) graph of a single antenna element is displayed in Fig. 2. In the next step, a two-element array structure is formed with the objective of improving antenna gain and directivity, also shown in Fig. 2. By doing that, the maximum gain is increased from 4.5 dB to 7.4 dB. The inter-elements distance is carefully selected in order to get the same wide bandwidth and directed beam.

Finally, the two elements array is converted into a MIMO system and adjusted so that each array in the MIMO system also covers a wide bandwidth from 24 GHz to 51 GHz, as depicted in Fig. 6. The reflection coefficient curves S_{11}, S_{22}, S_{33}, and S_{44} with values less than -10 dB match well with each other which satisfies the wide bandwidth requirements of mm-wave communication application. Also, the transmission coefficients (S_{12}, S_{13}, S_{14}) indicate decent isolation among the proposed MIMO antenna arrays as shown in Fig. 7. The isolation of more than 24 dB is noted among the arrays in the MIMO.

3.2. Radiation Patterns

The measurement setup adopted for radiation patterns consists of an anechoic chamber containing a horn antenna transmitter source and a Diamond-engineering Automated Measurement System (DAMS) which is supported by driving software. Furthermore, the real-time radiation patterns data is recorded with the help of a turn-table mechanism. The far-field radiation pat-

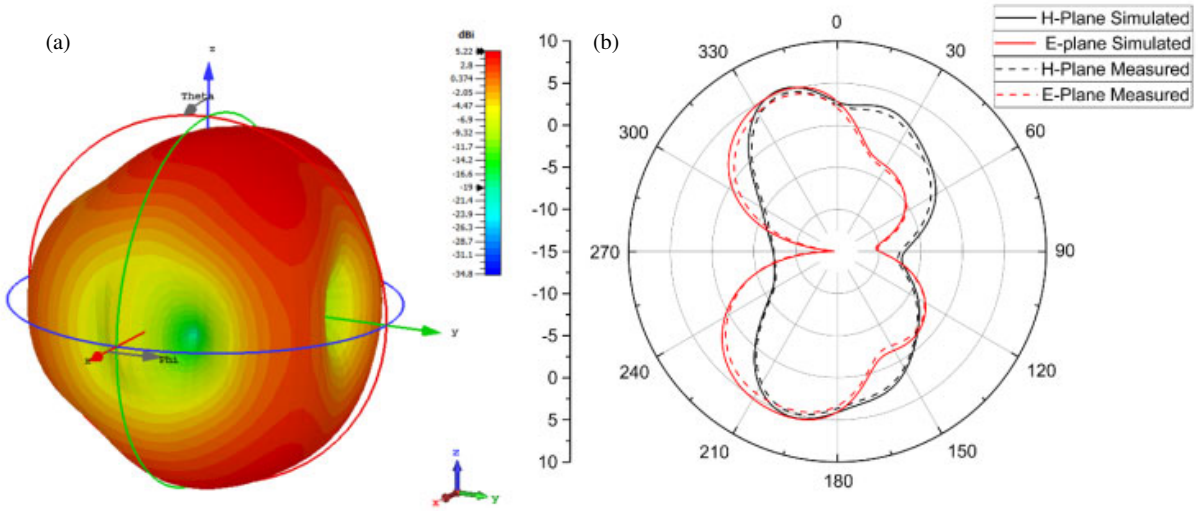

FIGURE 8. Radiation patterns of port 1 at 28 GHz, (a) in 3D shape, (b) at Phi $= 0^\circ$ (red) and 90° (black).

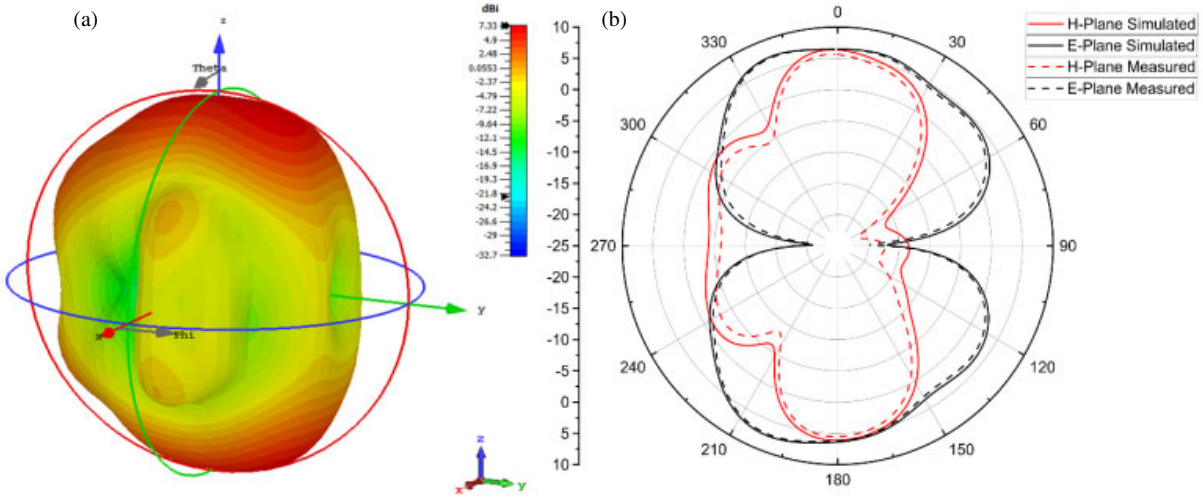

FIGURE 9. Radiation patterns of port 1 at 38 GHz, (a) in 3D shape, (b) at Phi $= 0^\circ$ (red) and 90° (black).

terns at Phi $= 0^\circ$ and Phi $= 90^\circ$ for port 1 are obtained at 28 GHz and 38 GHz for the proposed mm-wave MIMO antenna system and are shown in Figs. 8(a) and 9(a), respectively. The radiation patterns are bi-directional in the entire operational frequency band. Furthermore, the main lobes are found more to contribute in high radiation efficiency. Such an antenna design with good results is a suitable choice for mm-wave wireless applications and could be anticipated in 5G communication. The 2D radiation patterns at 28 GHz and 38 GHz are also shown in Figs. 8(b) and 9(b), respectively.

These remarkable features with the benefits of design simplicity and easy expansion to large-scale antenna system make the proposed design suitable for mm-wave communications.

3.3. Gain and Radiation Efficiency

The simulated realized gain associated with the entire operational frequency of the proposed MIMO antenna structure is found by CST software, which gives a good gain graph due to the array, as shown in Fig. 11. Result shows that the proposed antenna delivers a maximum gain of 7.4 dBi at 48 GHz in the entire operating band of interest. The gain values lie in the range of 4.2 to 7.4 dBi and provide 5.2 dB, 7.2 dB, and

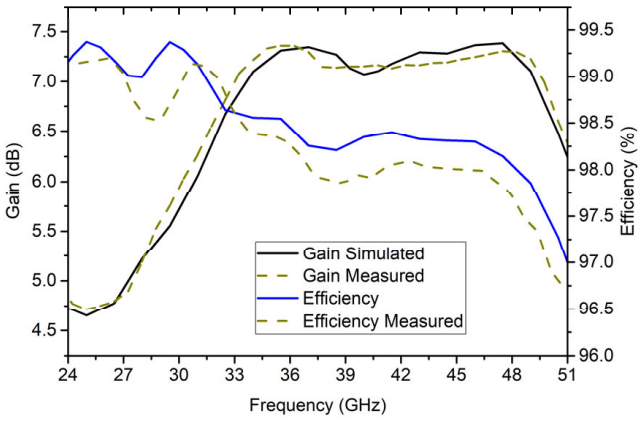

FIGURE 10. The simulated and measured realized gain and radiation efficiency graphs.

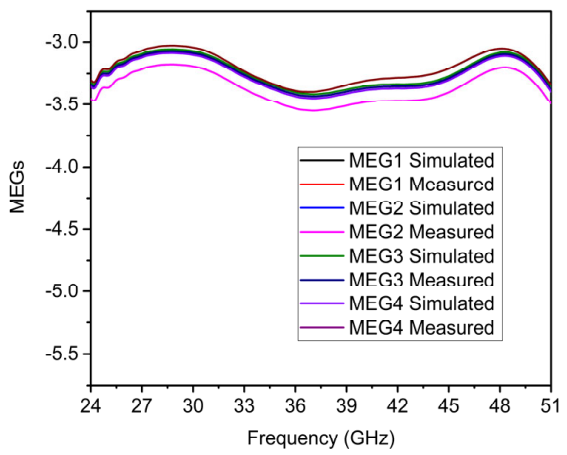

FIGURE 11. MEG (dB) between elements.

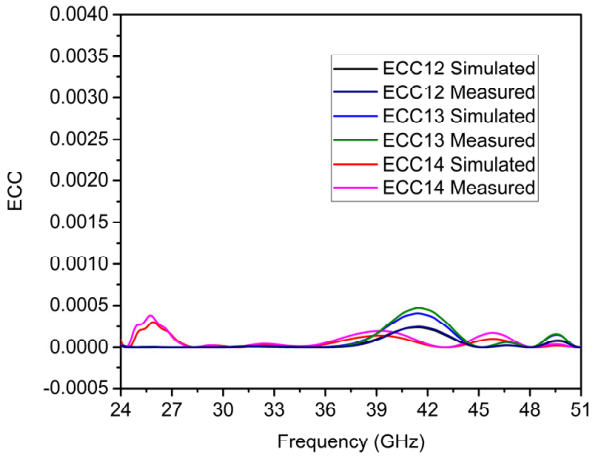

FIGURE 12. ECC graphs between elements.

7.4 dB gains at frequencies 28 GHz, 38 GHz, and 48 GHz, respectively. Due to the use of a Rogers 5880 dielectric substrate with a loss tangent of 0.0009, the low value of loss tangent contributes to achieving high efficiency; hence, the MIMO design offers high radiation efficiency of more than 96% over a wide bandwidth, which is a big achievement and makes it suitable for mm-wave bands applications. The simulated and measured radiation efficiency graphs are also shown in Fig. 10.

4. MIMO PERFORMANCE METRICS FOR THE PROPOSED ANTENNA

The proposed design is a Multiple-Input Multiple-Output (MIMO) antenna system. Therefore, it is important to investigate not only the antenna's fundamental characteristics but also various diversity parameters. Some of the important diversity performance parameters, ECC, DG, MEG, and CCL, were investigated, which determined the proposed MIMO antenna system to be a good candidate for mm-wave applications. These performance parameters are discussed one by one below.

4.1. Mean Effective Gain (MEG)

In order to acquire the received power characteristics and maximum diversity performance of the MIMO system in propagation environments, the Mean Effective Gain (MEG) is a significant MIMO performance parameter to realize a balanced power standard of the MIMO system and diversity performance with a good channel characteristic compared to an isotropic antenna in a multi-path channel [30, 31].

Mean effective gain (MEG) is the ratio of the received power to the incident power of the antenna in the multi-path environment. The maximum value of MEGs should be less than -3 dB [20, 30], and a value close to -3 dB is considered good. The proposed 4-port MIMO antenna provides very good MEG values, as depicted in Fig. 11. It can be represented with the help of the expressions below (2).

$$\mathrm{MEG}_i = 0.5\left(1 - \sum_{j=1}^{N} |S_{ij}|^2\right) \tag{2}$$

where N is the total number of antennas in MIMO system, i the ith antenna port, and j the reference jth antenna port.

4.2. Envelope Correlation Coefficient (ECC) and Diversity Gain (DG)

Envelope Correlation Coefficient represents the level of interference between radiation patterns of antennas in a MIMO system. The ideal value of ECC is 0; however, the acceptable value of ECC should be less than 0.05 for practical applications [32, 33]. In particular, the higher the ECC value is, the higher the interference will be. On the other hand, the lower the ECC is, the better the diversity performance of a MIMO system is. The anticipated ECC response is found acceptable all over the desired band, which means that the proposed MIMO antenna is effective. The ECC is calculated from radiation patterns, it can also be calculated from scattering transmission coefficients; the latter method is selected to calculate the ECC for the proposed MIMO antenna.

Diversity gain (DG) describes the communication link reliability as it determines the channel fading in the combination of two or more independent antennas. The DG value close to 10 dB or 10 dB is considered good. DG is inversely proportional to ECC, and its values can be calculated from ECC. Based on the requirements of practical standards, the DG value should be more than 9.95 dB. The DG value of the proposed MIMO antenna is much closer to the ideal value, which confirms that the interference is low among the elements, showing optimal diversity performance. ECC and DG are given in Fig. 12 and Fig. 13 and are calculated from Equations (3) and (4), respectively.

$$\mathrm{ECG}_{12} = \frac{|S_{11}^* S_{12} + S_{21}^* S_{22}|^2}{\left(1 - |S_{11}|^2 - |S_{21}|^2\right)\left(1 - |S_{22}|^2 - |S_{12}|^2\right)} \tag{3}$$

and

$$\mathrm{DG}_{ij} = 10 \times \sqrt{1 - \mathrm{ECC}_{ij}} \tag{4}$$

where S_{ij} represents the scattering parameter and shows the transmitted power from port j to port i.

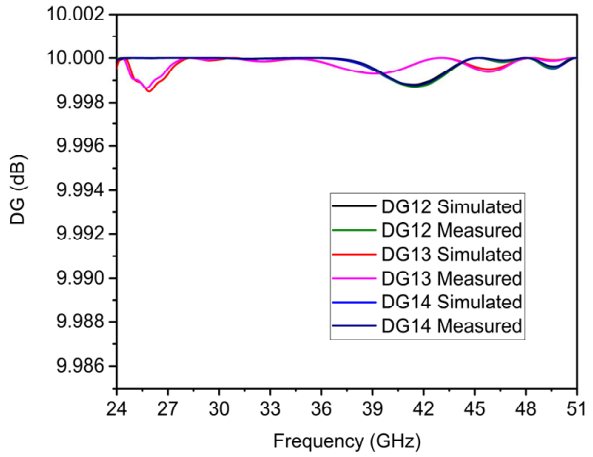

FIGURE 13. DG graphs between elements.

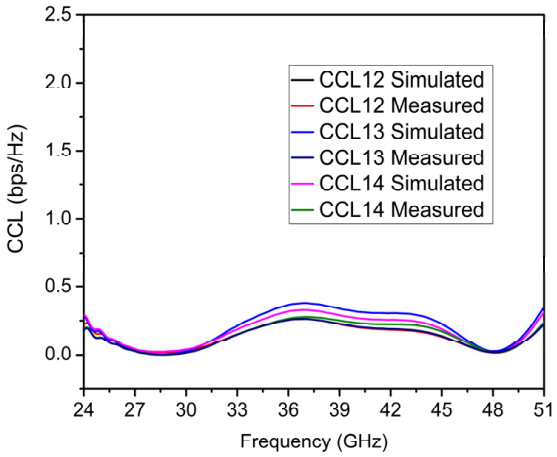

FIGURE 14. CCL graphs between elements.

TABLE 2. Comparison with other research works.

Refs.	Ports	Dimensions	BW (GHz)	Gain (dB)	Efficiency (%)	Isolation (dB)
[35]	2×2	$20 \times 24\,\text{mm}^2$	27.6–28.4/37.9–38.5	7.9	85	28
[36]	2×2	$47.5 \times 32.5\,\text{mm}^2$	37–40	6.5	80	25
[37]	2×2	$24 \times 22.5\,\text{mm}^2$	27.4–40	9	42	30
[38]	2×2	$110 \times 55\,\text{mm}^2$	27–28/37.2–38.8	7.95/8.27	89.89/88.25	30/24
[39]	1×2	$18 \times 36\,\text{mm}^2$	3–40	6	-	20
[40]	2×2	$24 \times 24\,\text{mm}^2$	24.2–37.8	6.4	91	27
[41]	2×2	$30 \times 30\,\text{mm}^2$	26–29	6.5	85	25
[42]	2×2	$24 \times 24\,\text{mm}^2$	23.6–31.5	5.66	85	27.5
[43]	1×2	$30 \times 15\,\text{mm}^2$	26.5–32.9	5	84	35
[44]	1×2	$14 \times 20\,\text{mm}^2$	17–25	6.5	80	16
[45]	4×4	$25 \times 25\,\text{mm}^2$	25.28–28.02	8.72	-	23.2
[46]	2×2	$55.27 \times 27.64\,\text{mm}^2$	27–40	5.5–8	84	25–30
[47]	4×4	$33 \times 33\,\text{mm}^2$	25–50	-	65–90	20
[48]	2×2	$26 \times 11\,\text{mm}^2$	26–28.2/36.2–42	5/5.7	99.5/98.6	30/25
Prop.	4×4	$18 \times 18\,\text{mm}^2$	24–51	7.4	96	25

4.3. Channel Capacity Loss (CCL)

CCL accounts for a maximum attainable limit of communication when a signal transmits completely, without communication channel loss. The channel capacity specifies the maximum transmission rate of information through a communication channel. The unit of CCL is bits/s/Hz, and the loss in channel capacity should not be greater than 0.4 bits/s/Hz for the entire band of interest; a low CCL indicates that the channel is used efficiently [34]. Fig. 14 shows the CCL graph, and in terms of S-parameters, it is represented by Equation (5).

$$\text{CCL}_{ij} = -\log_2 \det|\Psi^R| \tag{5}$$

where

$$\Psi^R = \begin{bmatrix} \Phi_{ii} & \Phi_{ij} \\ \Phi_{ji} & \Phi_{jj} \end{bmatrix}$$

and

$$\Phi_{ii} = 1 - \left(|S_{ii}|^2 + |S_{ij}|^2\right)$$
$$\Phi_{ij} = S_{ii}^* S_{ij} + S_{ji}^* S_{ij}$$

where S_{ij} represents the scattering parameter and shows the transmitted power from port j to port i.

5. COMPARISON WITH RECENT WORK

In the published literature, various MIMO antenna designs have been adopted; a comparison with existing research is presented in Table 2. This comparison takes into account key factors such as antenna dimensions, operating bandwidth, gain, efficiency, and isolation among MIMO elements. This proposed design has considerable good gain with high bandwidth and efficiency, and the comparison is provided in Table 2. In order to assess the performance, the antenna in [44] features a smaller antenna size but at the expense of limited bandwidth, low gain and effi-

ciency. Similarly, the antennas are concerned with larger size in [36, 38, 41, 46] and low-efficiency performances. Additionally, [35, 37, 45] offer the advantage of high peak gain but are restricted to low bandwidth. In contrast, the proposed MIMO design emphasizes significant isolation and offers an impressive operational bandwidth range of 24 to 51 GHz, adequate size, improved peak isolation, and high efficiency.

6. CONCLUSION

MIMO antennas are quite responsible in order to improve the coverage range, increase the channel capacity, and provide quality of service when being employed in any wireless communication system. In addition, millimeter-wave frequencies offer significant advantages such as high data rates, low latency, and extensive bandwidth. In order to achieve the desired data rates and meet bandwidth targets, the utilization of a MIMO configuration in mm-wave antenna design has the potential to enhance system performance. This proposed simple designed four-port MIMO array antenna offers wideband (24–51 GHz) with enhanced gain (7.4 dB), high efficiency (96%), and bi-directional radiation characteristics. Work on the design of mm-wave antennas has been done, and the extremely high bandwidth with good gain and optimal MIMO diversity performance parameters make the proposed design exceptional. The MIMO antenna exhibits good isolation of more than 22 dB against electromagnetic interaction, which demonstrates low mutual coupling. Furthermore, the comparisons between simulated and measured results ensured a good agreement. The MIMO performance metrics were also evaluated and are found in well-accepted ranges. The ECC, MEG, DG, and CCL give values of < 0.0005, < 3 dB, > 9.99 dB, and < 0.4 bits/s/Hz, respectively. Overall, the proposed wideband MIMO antenna is much more suitable for mm-wave 5G applications. In the future, the incorporation of a metasurface under the ground plane will further improve the gain and make the radiation pattern of the proposed design unidirectional. Moreover, the incorporation of a beam steering feature will make the proposed antenna system capable of wide area coverage for communication.

ACKNOWLEDGEMENT

Supported by National Nature Science Foundation of China (Grant No. 62174148), National Key Research and Development Program (NKRDP Grant No. 2022YFE0112000), Key Program for International Joint Research of Henan Province (Grant No. 231111520300).

REFERENCES

[1] Sharawi, M. S., "Current misuses and future prospects for printed multiple-input, multiple-output antenna systems [Wireless Corner]," *IEEE Antennas and Propagation Magazine*, Vol. 59, No. 2, 162–170, 2017.

[2] Li, X. and Z.-P. Nie, "Effect of array orientation on performance of MIMO wireless channels," *IEEE Antennas and Wireless Propagation Letters*, Vol. 3, 368–371, 2004.

[3] Khalily, M., R. Tafazolli, P. Xiao, and A. A. Kishk, "Broadband mm-Wave microstrip array antenna with improved radiation characteristics for different 5G applications," *IEEE Transactions on Antennas and Propagation*, Vol. 66, No. 9, 4641–4647, 2018.

[4] Niu, Y., Y. Li, D. Jin, L. Su, and A. V. Vasilakos, "A survey of millimeter wave communications (mmWave) for 5G: Opportunities and challenges," *Wireless Networks*, Vol. 21, 2657–2676, 2015.

[5] Zhang, J., X. Yu, and K. B. Letaief, "Hybrid beamforming for 5G and beyond millimeter-wave systems: A holistic view," *IEEE Open Journal of the Communications Society*, Vol. 1, 77–91, 2019.

[6] Kiani, S. H., A. Altaf, M. Abdullah, F. Muhammad, N. Shoaib, M. R. Anjum, R. Damaševičius, and T. Blažauskas, "Eight element side edged framed MIMO antenna array for future 5G smart phones," *Micromachines*, Vol. 11, No. 11, 956, 2020.

[7] Khan, M. M., K. Islam, M. N. A. Shovon, M. Baz, and M. Masud, "Design of a novel 60 GHz millimeter wave Q-slot antenna for body-centric communications," *International Journal of Antennas and Propagation*, Vol. 2021, No. 1, 9795959, 2021.

[8] Long, Y., Z. Chen, and J. Fang, "Nonasymptotic analysis of capacity in massive MIMO systems," *IEEE Wireless Communications Letters*, Vol. 4, No. 5, 541–544, 2015.

[9] Li, Z., R. Jian, Y. Chen, and T. Chen, "A novel design for millimeter wave microstrip antenna with bandwidth enhancement," in *2018 IEEE Student Conference on Research and Development (SCOReD)*, 1–4, Selangor, Malaysia, 2018.

[10] Tong, K.-F. and T.-P. Wong, "Circularly polarized U-slot antenna," *IEEE Transactions on Antennas and Propagation*, Vol. 55, No. 8, 2382–2385, 2007.

[11] Aliakbari, H., A. Abdipour, R. Mirzavand, A. Costanzo, and P. Mousavi, "A single feed dual-band circularly polarized millimeter-wave antenna for 5G communication," in *2016 10th European Conference on Antennas and Propagation (EuCAP)*, 1–5, Davos, Switzerland, 2016.

[12] Kamal, M. M., S. Yang, S. H. Kiani, M. R. Anjum, M. Alibakhshikenari, Z. A. Arain, A. A. Jamali, A. Lalbakhsh, and E. Limiti, "Donut-shaped mmWave printed antenna array for 5G technology," *Electronics*, Vol. 10, No. 12, 1415, 2023.

[13] Elftouh, H., N. A. Touhami, M. Aghoutane, S. E. Amrani, A. T. Puente, and M. Boussouis, "Miniaturized microstrip patch antenna with defected ground structure," *Progress In Electromagnetics Research C*, Vol. 55, 25–33, 2014.

[14] Khan, M. I., M. I. Khattak, S. U. Rahman, A. B. Qazi, A. A. Telba, and A. Sebak, "Design and investigation of modern UWB-MIMO antenna with optimized isolation," *Micromachines*, Vol. 11, No. 4, 432, 2020.

[15] Ahmad, G. and A. Ullah, "Wide dual band MIMO patch antenna for future 5G applications," *Journal of Space Technology*, Vol. 10, No. 1, 7–12, 2020.

[16] Jilani, S. F., Q. H. Abbasi, M. A. Imran, and A. Alomainy, "Design and analysis of millimeter-wave antennas for the fifth generation networks and beyond," *Wiley 5G Ref: The Essential 5G Reference Online*, 1–21, 2019.

[17] Zaidi, N. I., N. H. A. Rahman, M. F. Yahya, M. S. A. Nordin, S. Subahir, Y. Yamada, and A. Majumdar, "Analysis on bending performance of the electro-textile antennas with bandwidth enhancement for wearable tracking application," *IEEE Access*, Vol. 10, 31 800–31 820, 2022.

[18] Ferreira, D., P. Pires, R. Rodrigues, and R. F. S. Caldeirinha, "Wearable textile antennas: Examining the effect of bending on their performance," *IEEE Antennas and Propagation Magazine*, Vol. 59, No. 3, 54–59, 2017.

[19] Strinati, E. C., S. Barbarossa, J. L. Gonzalez-Jimenez, D. Ktenas, N. Cassiau, L. Maret, and C. Dehos, "6G: The next frontier: From holographic messaging to artificial intelligence using subterahertz and visible light communication," *IEEE Vehicular Technology Magazine*, Vol. 14, No. 3, 42–50, 2019.

[20] Ma, P.-P., F.-F. Fan, and X.-Y. Zhao, "Broadband dual-frequency high isolation base station antenna with low RCS structure loaded," *Applied Computational Electromagnetics Society Journal (ACES)*, Vol. 39, No. 3, 268–274, Mar. 2024.

[21] Rajendran, D., R. Subramaniam, and R. K. Dhandapani, "Performance analysis of eight-element MIMO mobile phone antenna for sub-6 GHz 5G applications," *Applied Computational Electromagnetics Society Journal (ACES)*, Vol. 39, No. 4, 319–326, Apr. 2024.

[22] Zhu, F. G., J. D. Xu, and Q. Xu, "Reduction of mutual coupling between closely-packed antenna elements using defected ground structure," in *2009 3rd IEEE International Symposium on Microwave, Antenna, Propagation and EMC Technologies for Wireless Communications*, 1–4, Beijing, China, 2009.

[23] Assimonis, S. D., T. V. Yioultsis, and C. S. Antonopoulos, "Computational investigation and design of planar EBG structures for coupling reduction in antenna applications," *IEEE Transactions on Magnetics*, Vol. 48, No. 2, 771–774, 2012.

[24] Zhang, X., Z. Li, A. Zhan, and Y. Mei, "Design of a reconfigurable band-notched wideband antenna using EBG structures," *Applied Computational Electromagnetics Society Journal (ACES)*, Vol. 38, No. 11, 895–902, Nov. 2023.

[25] Su, S.-W., C.-T. Lee, and F.-S. Chang, "Printed MIMO-antenna system using neutralization-line technique for wireless USB-dongle applications," *IEEE Transactions on Antennas and Propagation*, Vol. 60, No. 2, 456–463, 2012.

[26] Ou, Y., X. Cai, and K. Qian, "Two-element compact antennas decoupled with a simple neutralization line," *Progress In Electromagnetics Research Letters*, Vol. 65, 63–68, 2017.

[27] Zhang, Z., M. F. Iskander, J.-C. Langer, and J. Mathews, "Dual-band WLAN dipole antenna using an internal matching circuit," *IEEE Transactions on Antennas and Propagation*, Vol. 53, No. 5, 1813–1818, 2005.

[28] Chen, Z., Z. Wang, F. Chen, X. Hou, Y. Zhou, and L. Phav, "High-isolation Wi-Fi antenna system based on metamaterial," *Applied Computational Electromagnetics Society Journal (ACES)*, Vol. 38, No. 5, 343–351, May 2023.

[29] Bhatia, S. S., J. S. Sivia, and N. Sharma, "An optimal design of fractal antenna with modified ground structure for wideband applications," *Wireless Personal Communications*, Vol. 103, No. 3, 1977–1991, 2018.

[30] Correia, L. M., *Wireless Flexible Personalized Communications*, 482, John Wiley & Sons, Inc., United States, 2001.

[31] Glazunov, A. A., A. F. Molisch, and F. Tufvesson, "Mean effective gain of antennas in a wireless channel," *IET Microwaves, Antennas & Propagation*, Vol. 3, No. 2, 214–227, Apr. 2009.

[32] Parvathi, K. S. L. and S. R. Gupta, "Novel dual-band EBG structure to reduce mutual coupling of air gap based MIMO antenna for 5G application," *AEU — International Journal of Electronics and Communications*, Vol. 138, 153902, 2021.

[33] Kulkarni, J., A. Desai, and C.-Y. D. Sim, "Wideband four-port MIMO antenna array with high isolation for future wireless systems," *AEU — International Journal of Electronics and Communications*, Vol. 128, 153507, 2021.

[34] Aghoutane, B., S. Das, M. E. Ghzaoui, B. T. P. Madhav, and H. E. Faylali, "A novel dual band high gain 4-port millimeter wave MIMO antenna array for 28/37 GHz 5G applications," *AEU — International Journal of Electronics and Communications*, Vol. 145, 154071, 2022.

[35] Raheel, K., A. Altaf, A. Waheed, S. H. Kiani, D. A. Sehrai, F. Tubbal, and R. Raad, "E-shaped H-slotted dual band mmWave antenna for 5G technology," *Electronics*, Vol. 10, No. 9, 1019, 2021.

[36] Sehrai, D. A., M. Asif, N. Shoaib, M. Ibrar, S. Jan, M. Alibakhshikenari, A. Lalbakhsh, and E. Limiti, "Compact quad-element high-isolation wideband MIMO antenna for mm-Wave applications," *Electronics*, Vol. 10, No. 11, 1300, 2021.

[37] Patel, A., A. Vala, A. Desai, I. Elfergani, H. Mewada, K. Mahant, C. Zebiri, D. Chauhan, and J. Rodriguez, "Inverted-L shaped wideband MIMO antenna for millimeter-wave 5G applications," *Electronics*, Vol. 11, No. 9, 1387, 2022.

[38] Marzouk, H. M., M. I. Ahmed, and A. H. A. Shaalan, "Novel dual-band 28/38 GHz MIMO antennas for 5G mobile applications," *Progress In Electromagnetics Research C*, Vol. 93, 103–117, 2019.

[39] Khan, M. I., M. I. Khattak, S. U. Rahman, A. B. Qazi, A. A. Telba, and A. Sebak, "Design and investigation of modern UWB-MIMO antenna with optimized isolation," *Micromachines*, Vol. 11, No. 4, 432, 2020.

[40] Khan, M. A., A. G. A. Harbi, S. H. Kiani, A. N. Nordin, M. E. Munir, S. I. Saeed, J. Iqbal, E. M. Ali, M. Alibakhshikenari, and M. Dalarsson, "mmWave four-element MIMO antenna for future 5G systems," *Applied Sciences*, Vol. 12, No. 9, 4280, 2022.

[41] Rahman, S., X.-C. Ren, A. Altaf, M. Irfan, M. Abdullah, F. Muhammad, M. R. Anjum, S. N. F. Mursal, and F. S. AlKahtani, "Nature inspired MIMO antenna system for future mmWave technologies," *Micromachines*, Vol. 11, No. 12, 1083, 2020.

[42] Khan, M. I., S. Khan, S. H. Kiani, N. O. Parchin, K. Mahmood, U. Rafique, and M. M. Qadir, "A compact mmWave MIMO antenna for future wireless networks," *Electronics*, Vol. 11, No. 15, 2450, 2022.

[43] Hussain, N., W. A. Awan, W. Ali, S. I. Naqvi, A. Zaidi, and T. T. Le, "Compact wideband patch antenna and its MIMO configuration for 28 CST Microwave Studio, ver. 2008," Computer Simulation Technology, Framingham, MA, 2008.

[44] Sehrai, D. A., M. Asif, J. Khan, M. Abdullah, W. A. Shah, S. Alotaibi, and N. Ullah, "A high-gain and wideband MIMO antenna for 5G mm-wave-based IoT communication networks," *Applied Sciences*, Vol. 12, No. 19, 9530, 2022.

[45] Güler, C. and S. E. B. Keskin, "A novel high isolation 4-port compact MIMO antenna with DGS for 5G applications," *Micromachines*, Vol. 14, No. 7, 1309, 2023.

[46] Megahed, A. A., E. H. Abdelhay, M. Abdelazim, and H. Y. M. Soliman, "5G millimeter wave wideband MIMO antenna arrays with high isolation," *EURASIP Journal on Wireless Communications and Networking*, Vol. 2023, No. 1, 61, 2023.

[47] Abbas, M. A., A. Allam, A. Gaafar, H. M. Elhennawy, and M. F. A. Sree, "Compact UWB MIMO antenna for 5G millimeter-wave applications," *Sensors*, Vol. 23, No. 5, 2702, 2023.

[48] Ali, W., S. Das, H. Medkour, and S. Lakrit, "Planar dual-band 27/39 GHz millimeter-wave MIMO antenna for 5G applications," *Microsystem Technologies*, Vol. 27, 283–292, Jul. 2020.